High current density via direct electron transfer by the halophilic anode respiring bacterium Geoalkalibacter subterraneus

Alessandro Carmona Martinez, Mélanie Pierra, Eric Trably, Nicolas Bernet

Carmona Martinez, A., Pierra, M., Trably, E., and Bernet, N. 2013. Physical Chemistry Chemical Physics, 15(45):19699 - 19707. http://dx.doi.org/10.1039/c3cp54045f

High current density via direct electron transfer by the halophilic anode respiring bacterium *Geoalkalibacter subterraneus*

Alessandro A. Carmona-Martínez*, Mélanie Pierra, Eric Trably and Nicolas Bernet

INRA, UR0050, Laboratoire de Biotechnologie de l'Environnement, Avenue des Etangs, Narbonne, F-11100, France

Keywords: *Geoalkalibacter subterraneus*, Bioelectrochemical systems, Cyclic voltammetry, Confocal Laser Scanning Microscopy, Direct electron transfer

*author of correspondence; phone: +33 (0) 4 68 42 51 62; fax: +33 (0)4 68 42 51 60, email to: alessandro.carmona@supagro.inra.fr

Abstract

In this study the characterization of *Geoalkalibacter subterraneus* is presented, a novel halophilic anode respiring bacteria (ARB) previously selected and identified in a potentiostically controlled bioelectrochemical system (BES) inoculated with sediments from a salt plant. Pure culture electroactive biofilms of *Glk. subterraneus* were grown during chronoamperometric batch experiments at a graphite electrode poised at +200 mV (vs. SCE) with 10 mM acetate as electron donor. These biofilms exhibited the highest current density (4.68 ± 0.54 A/m^2) reported on a planar material with a pure culture under saline conditions (3.5% NaCl). To investigate possible anodic electron transfer (ET) mechanisms, cyclic voltammetry (CV) of mature visible apparent reddish biofilms was performed under bioelectrocatalytic substrate consumption (turnover) and in absence of substrate (non-turnover). CV evidenced a well defined typical sigmoidal shape and a pair of clear redox couples under turnover and non-turnover conditions, respectively. Moreover, the calculation of their formal potentials indicated the presence of a common ET mechanism present in both CV conditions between -427.6 ± 0.5 ($E_{f,2}$) and -364.8 ± 4.5 mV ($E_{f,3}$). Confocal laser scanning microscopy inspection showed a biofilm structure composed of several layers of metabolically active bacteria that spread all over the electrode material within a biofilm up to 76 ± 7 µm thick. Such value, high for the thickness normally reported in the literature for pure culture electroactive bacteria justifies further investigations. Taken together, these results suggest that *Glk. subterraneus* performs a direct ET mechanism in contact with the electrode material. Furthermore, direct current generation from saline wastewaters significantly expands the application of BESs.

1. Introduction

Bioelectrochemical systems (BESs) are a group of technologies derived from the bidirectional electron transfer (ET) interactions between microorganisms and electrode materials[1]. More specifically: 1) the harvest of electrons from the oxidation of a substrate and their further transfer to an electrode (*e.g.*, for the direct production of electricity[2]) and 2) the uptake of electrons from the electrode material to reduce a substrate for the production of valuable industrial products such as hydrogen gas[3], sodium hydroxide or acetate[4]. Up to now, two main microbial ET mechanisms have been extensively described: direct electron transfer (DET) and mediated electron transfer (MET). Whereas in DET bacteria need to be in direct contact with the electrode material to release/accept electrons via c-type cytochromes[5], in MET bacteria are capable of releasing/accepting electrons via self produced redox mediator molecules such as flavins[6] or phenazines[7] (among others[8-11]). Although microbial ET mechanisms in BESs have been extensively studied in two model bacteria families such as *Geobacteraceae* and *Shewanaellaceae*[1], there are many other bacteria capable of donating/accepting electrons to/from an electrode (see Table S1).

While members of the *Geobacteraceae* family are capable of performing a DET mechanism, with significant current densities (up to 9 A/m^2)[12] and forming thick biofilms (about 50 um[13-18]) in freshwater environments, *Shewanaellaceae* is capable of performing both DET and MET mechanisms. Interestingly, *Shewanaellaceae* produces very low current densities[19], likely due to their limitation to form thin-monolayer biofilms on the electrode surface[20, 21]. Although their ET mechanisms are extensively understood, there is still a great interest to identify and characterize other bacteria capable of forming electroactive biofilms and producing significant current densities since they can aid to comprehend more precisely how ET occurs through different microbial species[22, 23]. Furthermore, direct current generation from saline wastewaters as the ones produced in the sea-food, petroleum and leather industries could significantly broad the application of BESs.

For the characterization of electroactive bacteria diverse techniques are available. These techniques target practically all type of parameters, from architecture to electrochemistry of biofilms[24]. Here, the novel halophilic anode respiring bacterium (ARB) *Geoalkalibacter subterraneus* (henceforth, *Glk. subterraneus*) is characterized. *Glk. subterraneus* was previously selected and identified in a potentiostically controlled BES inoculated with sediments from a salt plant[25]. An electrochemical as well as a microscopic approach was employed. Chronoamperometry was used to evaluate *Glk. subterraneus*'s maximum current

density production with intermittent measurements of its ET mechanism by cyclic voltammetry and confocal laser scanning microscopy to analyze biofilm electrode coverage and thickness.

2 Results and discussion

2.1 Bioelectrochemical biofilm formation of *Geoalkalibacter subterraneus* and generation of high current density under saline conditions

Fig. 1 shows a representative chronoamperometric (CA) biofilm growth of *Glk. subterraneus* on a graphite planar electrode at an applied potential of +200 mV (vs. SCE) with 10 mM sodium acetate as the electron donor. For all CA biofilm growth experiments, strict anoxic conditions were procured as described in the Experimental section and routinely tested by gas chromatographic analysis since *Glk. subterraneus* preferentially grows under these conditions[26].

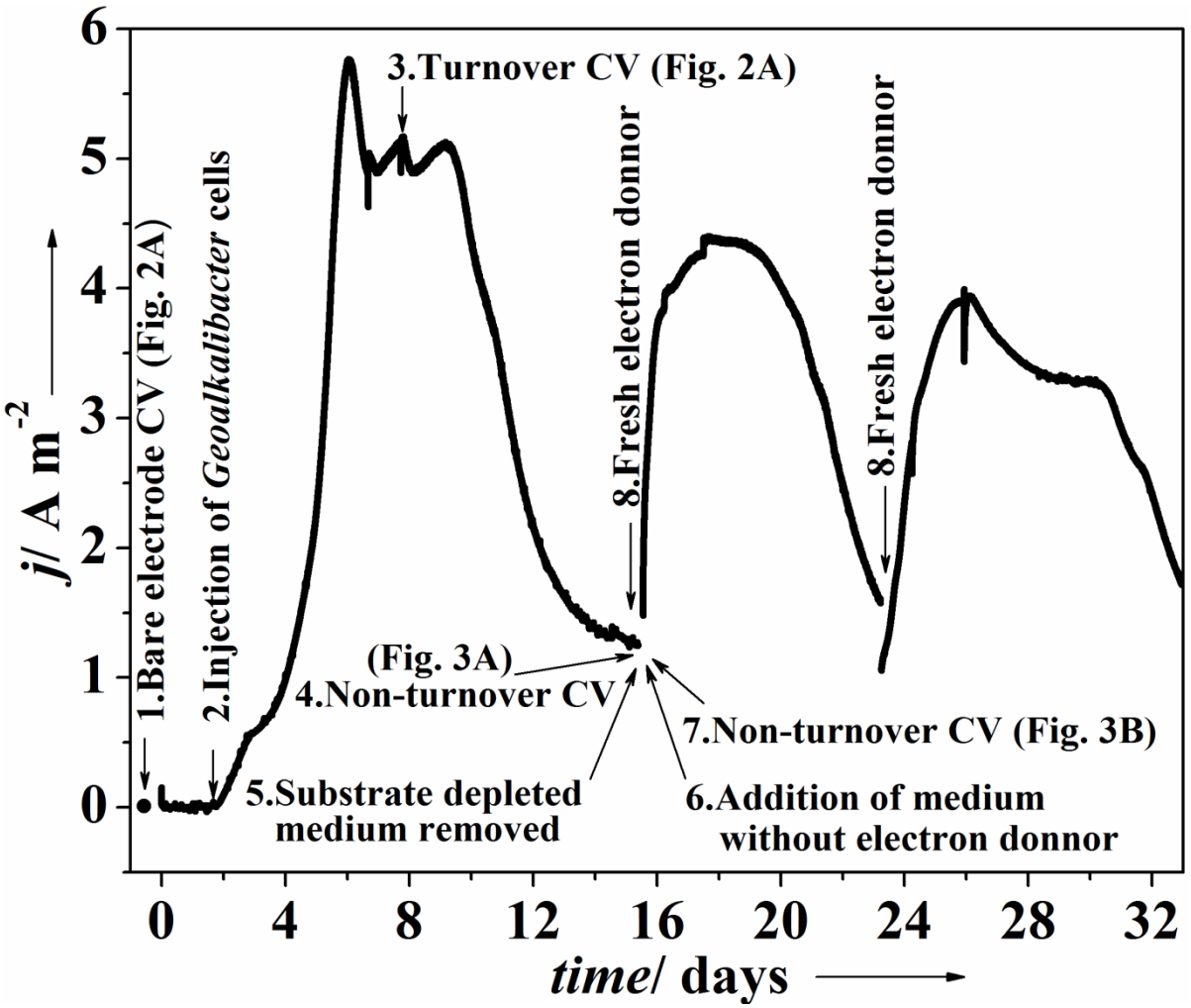

Fig. 1 Representative chronoamperometric fed-batch cycles of *Geoalkalibacter subterraneus* biofilms grown on graphite planar electrodes (15 cm^2); applied potential: +200 mV vs. SCE (KCl 3.0 M).

As denoted in Fig. 1, approximately after 24 h of poising the working electrode immersed in the growth medium, the electrochemical cell was inoculated and it took around 24 more hours for biofilm growth to begin. This was illustrated as an exponential-like current production trend, characteristic of ARB able to produce high currents and thick biofilms[27-29] (see Table S1). Fig. 1 shows that at day six of incubation, the current density peaked a maximum value (j_{max}) of about 5.7 A/m^2. This value establishes the highest current density produced by an ARB pure culture under saline conditions (3.5% NaCl)[30].

When comparing j_{max} by pure culture biofilms of *Glk.*, our results are consistent with previous observations in our group for biofilms enriched with *Geoalkalibacter* in potentiostically controlled BESs inoculated with sediments from a salt plant (j_{max}: 4.5 to 8.5 A/m^2)[31]. Furthermore, our results corroborate as well those of a recent publication by Miceli *et al.*, (2012)[32] showing *Geoalkalibacter* dominated biofilms derived from environmental anaerobic samples (j_{max}: 4.2 and 8.9 A/m^2). Similarly, Badalamenti *et al.* (2013)[30] reported the electrochemical performance of *Glk. subterraneus* grown on graphite rod electrodes under lower saline conditions (1.7% NaCl). They showed also a significant high j_{max} (3.3 A/m^2) but lower than the one reported here (5.7 A/m^2). One reason why current densities reported here were higher, could be the discrepancy between their and our experimental procedures (see Table S2); *e.g.*: higher concentration of salt (therefore increasing the conductivity of the electrolyte solution[33]), more positive applied potential (hence increasing biofilm formation[19]) and distance between working and counter electrodes due to BES architecture[34]. Nevertheless, in our experiments a lower concentration of electron donor (10 mM sodium acetate) generated higher current densities. A finding not totally consistent with literature data, since it has been extensively demonstrated that the current density augments by increasing the concentration of substrate until saturation kinetics[35, 36].

After the maximum current density was reached, a period of a stable current production was observed at 4.68 ± 0.54 A/m^2 (when both reproducible replicates are considered for the calculation, see Fig. S1). In between, CA was stopped and turnover CV was performed as indicated in the Experimental section. Around day nine, CA showed a sudden current decrease due to substrate exhaustion as confirmed at the end of the cycle by metabolite analysis. The conversion of substrate into current as coulombic efficiency (CE) was assessed by considering the ratio of electrons actually obtained from the substrate and the amount of electrons theoretically available[2]. Here, in semi-batch half-cell experiments, CE exceeded 100% (114 ± 14). This was likely due to oxidation of hydrogen produced at the cathode[37]

since a significant percentage (oxidizable by *Glk. subterraneus*[26]) was detected in the gas phase of our experiments (*e.g.*, the gas composition during CA at the maximum of current production was CO_2 16.6 %, H_2 82.2 %, O_2 1.05% and CH_4 0.34 %). The focus of this study was the characterization of *Glk. subterraneus* in terms of current output, electron transfer and biofilm formation and not maximizing CE as would be typical for applied BESs such as microbial fuel cells[2] or microbial electrolysis cells[3].

In several studies where electroactive bacteria are characterized as a pure culture, it has been usually found that in further batch CA cycles performed by media replenishment, the current recovers or exceeds its previous value[38-44]. As seen in Fig. 1, the current density did not recover its previous value after the substrate depleted media was replenished at the end of the first and second CA semi-batch cycles. On the other side, the immediate production of current can be considered a proof of bacteria's ability to convert the supplied substrate into current instead of using it for biosynthesis[45]. Therefore, this points out a possible direct electron transfer (DET) mechanism[23].

A similar phenomenon where current density does not recover its previous value was also observed elsewhere[22, 30, 46-52]. A possible explanation could be that the presence of a substance (or substances) produced in the previous CA cycle is required to achieve previous similar performance, hence hindering the biofilm to produce as much current density as in the previous CA cycle.

2.1.1 Comparison of *Geoalkalibacter subterraneus* and *Geobacter sulfurreducens* in terms of chronoamperometric current density production

To conduct an accurate comparison of the performance of *Glk. subterraneus*, parallel electrochemical experiments were carried out with the extensively well characterized[12, 53-60] model bacteria *Geobacter sulfurreducens* (hereafter, *Gb. sulfurreducens*). *Gb. sulfurreducens* was employed here as an appropriate reference of an ARB in terms of j_{max} obtained during CA experiments, analysis of its ET mechanism with cyclic voltammetry (CV) and biofilm examination with the use of confocal laser scanning microscopy (CLSM) under similar experimental conditions; *i.e.*: identical half-cell architecture and components, temperature, pH and applied potential.

Under our experimental conditions, *Gb. sulfurreducens* was able to produce a higher j_{max} (11.60 ± 2.21 A/m^2) than the one obtained with *Glk. subterraneus* (see Table S1 and Fig. S1). *Gb. sulfurreducens* biofilms obtained here produced results which corroborate previous

findings obtained by others with this model bacterium[12, 28, 29, 51, 61]. This confirms that: 1) our experimental methods are well standardized procedures comparable to the ones reported in the current literature and that 2) *Gb. sulfurreducens* is the ARB producing the highest current densities in a fresh water environment. In addition, a plausible reason why *Gb. sulfurreducens* biofilms outperformed *Glk. subterraneus* in terms of j_{max} is related to the diversified ET mechanism found in *Gb. sulfurreducens.* This is illustrated by the presence of several redox couples in CV and higher biofilm electrode coverage as per CLSM (see below).

2.2 Turnover CV analysis of *Geoalkalibacter subterraneus* in the presence of substrate

To analyze the extracellular electron transfer mechanism occurring in *Glk. subterraneus*, CV was performed during three different conditions as described in the Experimental section. Representative CVs for both conditions are shown in Fig. 2 (turnover) and Fig. 3 (non-turnover). As proof that the turnover and non-turnover CV signals are due to a biofilm formed at the electrode surface, a control CV of the bare surface electrode immersed in growth medium is included for comparison (dotted line in Fig. 2A and in Fig. 3A). The negative control CV showed no appreciable signals.

Fig. 2A shows a representative turnover CV illustrating a sigmoidal shape typically found in ARB able to produce high currents and thick biofilms like *Geobacter sulfurreducens* PCA[12], *Rhodopseudomonas palustris* DX-1[40], *Thermincola ferriacetica* DSMZ 14005[22] and more recently *Geoalkalibacter ferrihydriticus* DSM 17813[30]. Badalamenti *et al.*[30] reported the CV characterization of *Glk. subterraneus* biofilms but only under turnover conditions and showing a sigmoidal shape. The present observations of turnover CV analysis corroborate the findings of Badalamenti *et al.*[30]. However, the existing differences are very likely due to experimental procedures. When calculating the respective first derivative of the turnover CV of *Glk. subterraneus*, under our experimental turnover conditions, two different inflection points are revealed (Fig. 2B). A first inflection point with a formal potential ($E_{f,1}$) at -446.5 ± 1.2 and a second clearly prominent inflection point $E_{f,3}$ at -364.8 ± 4.5 mV (vs. SCE), a potential commonly ascribed to DET-proteins (see Fig S2). Likewise, multiple inflection points in the first derivative (here defined as $E_{f,1}$) have been reported elsewhere for other electroactive bacteria such as *Gb. sulfurreducens*[27, 51, 55, 61] and *T. ferriacetica*[41]. Nevertheless, it is not completely clear how these non prominent "additional" inflection points (such as $E_{f,1}$) are involved in the overall ET mechanism[51].

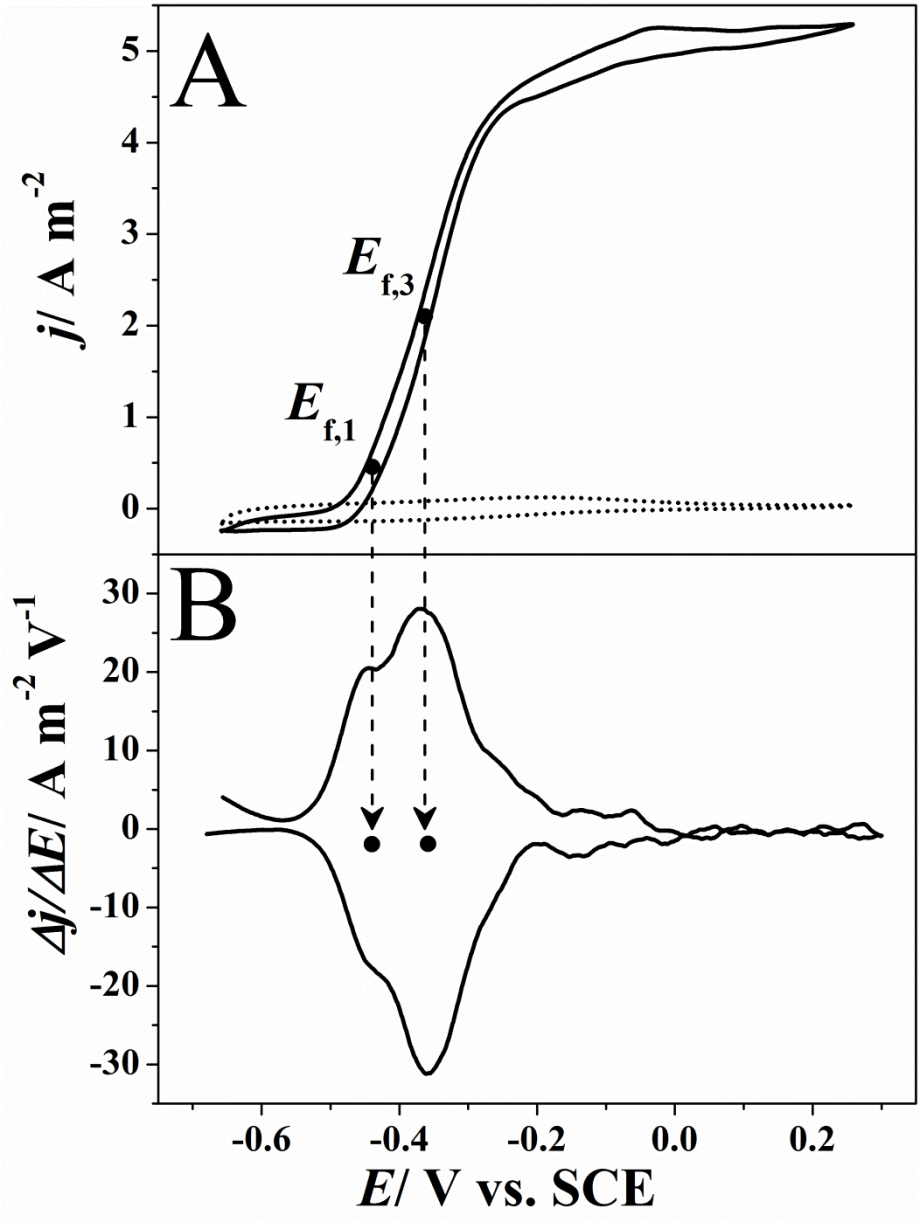

177

178 **Fig. 2** A) Representative turnover cyclic voltammogram of a *Geoalkalibacter subterraneus*
179 biofilm (continuous line) and B) respective first derivative curve. As well in A), dotted line
180 shows bare electrode CV performed before chronoamperometric biofilm growth.

181 When examining the turnover CV signal, it is clear that the CV shape shown here resembled
182 the one seen for bacteria capable of performing a DET mechanism via outer membrane
183 cytochromes (OMCs). Nevertheless, there is still no conclusive evidence whether OMCs are
184 responsible for a DET mechanism in the electroactive biofilms of *Glk. subterraneus*.
185 Moreover, the prominent inflection point potentials found here were very similar to the
186 potential found for DET (see Fig. S2). As shown in Fig. S2, bacteria able to perform a DET
187 mechanism presented an inflection point in a very broad potential window that ranged from -

500 to -300 mV vs. SCE. However these differences could be attributed to the particular growth conditions (*e.g.*, pH, temperature, substrate, salt concentration, among others).

2.2.1 Turnover CV comparison of *Geoalkalibacter subterraneus* and *Geobacter sulfurreducens* biofilms

Further evidence of a DET mechanism performed by *Glk. subterraneus* was provided by a comparative analysis conducted while performing electrochemical experiments to grow electroactive biofilms of *Gb. sulfurreducens* (see Fig. S1). Fig. S3 shows an exemplary turnover CV of a *Glk. subterraneus* biofilm compared to a turnover CV of a *Gb. sulfurreducens* biofilm. As expected, *Gb. sulfurreducens* illustrated the typical sigmoidal shape under turnover conditions obtained by others[12, 27, 51, 55, 61] and its first derivative showed as well two inflection points included in the potential window of $E_{f,1}$ and $E_{f,3}$ (see Fig. S3). This provides additional information on the ability of *Glk. subterraneus* to perform a DET mechanism and could indicate a similar ET process as in the case of *Gb. sulfurreducens*.

2.3 Non-turnover CV analysis of *Geoalkalibacter subterraneus* in the absence of substrate

Fig. 3 shows exemplary non-turnover CVs of a *Glk. subterraneus* biofilm. Fig. 3A shows a substrate-depleted CV when substrate was totally consumed (as per metabolite analysis) during CA cycle and Fig. 3B shows a substrate-deprived CV when the substrate depleted medium was replenished for fresh medium with no electron donor.

Both non-turnover CVs in Fig. 3A and B depict a very similar voltammogram shape. Additionally, both CVs possess two apparent redox couples with formal potentials $E_{f,2}$ and $E_{f,4}$. However, the substrate-depleted CV in Fig. 3A exhibits a catalytic behaviour with a limiting current of about 2 A/m^2. When compared to Fig. 3B, the limiting current masks the two redox couples that were clearly observed when CV was performed in total absence of electron donor (under substrate deprived non-turnover CV). The catalytic behaviour observed in Fig. 3A could be due to the presence of a substance (or substances) produced during CA. Interestingly, the observed catalytic current of 2 A/m^2 during non-turnover CV in Fig. 3A was in agreement with the current density observed at the end of the first CA cycle shown in Fig. 1 (residual current of about 1.3 A/m^2).

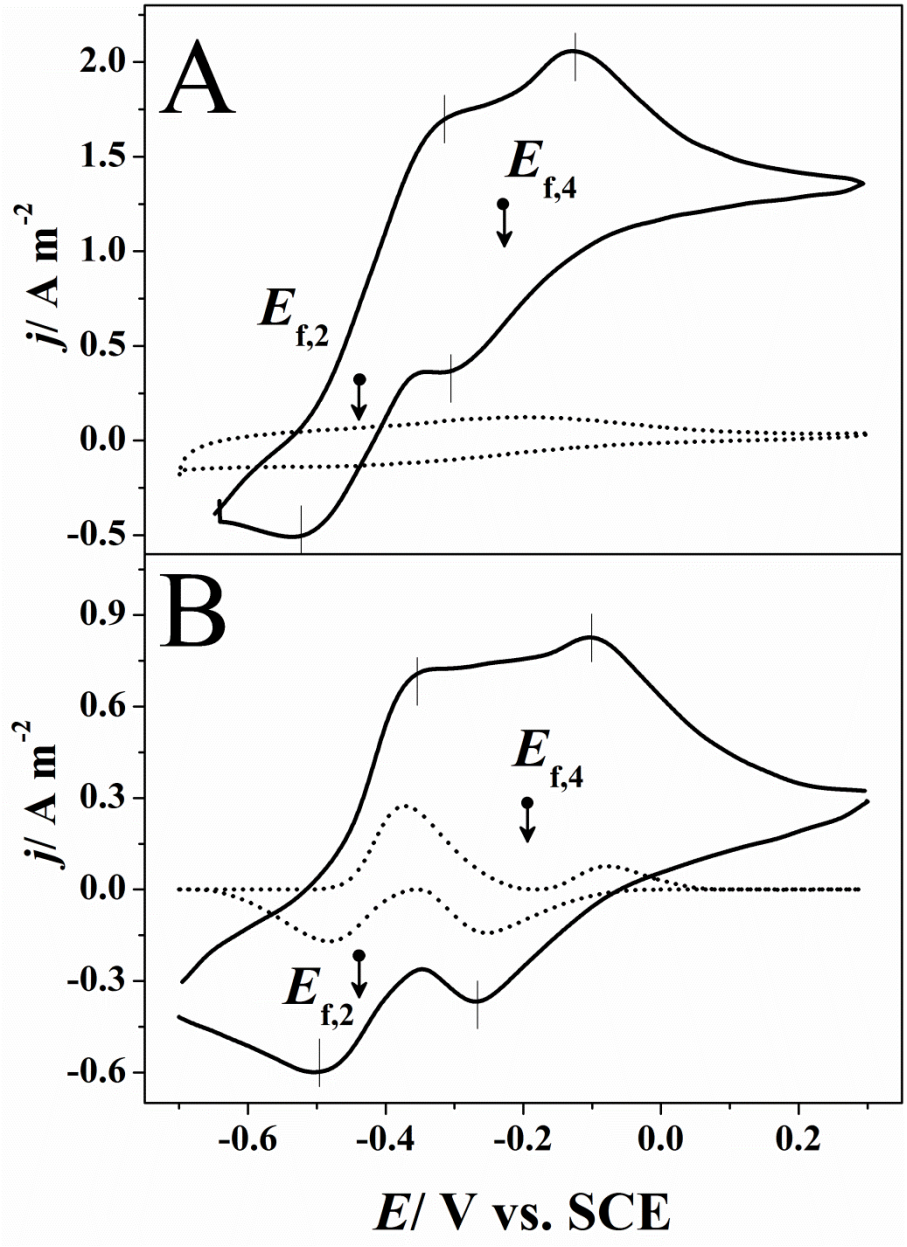

Fig. 3 A) Representative cyclic voltammogram of *Geoalkalibacter subterraneus* biofilm u substrate depleted conditions (continuous line) and cyclic voltammogram of bare electrode (dotted line); B) substrate deprived non-turnover cyclic voltammogram (dotted line provides the respective SOAS[62] base-line subtracted curve).

Fig. 3B shows the SOAS[62] base-line subtracted curve (dotted line) of the substrate deprived non-turnover CV (see Experimental section). The subtracted CV clearly depicts the position of two redox couples with formal potentials $E_{f,2}$ and $E_{f,4}$ at -427.6 ± 0.5 and -165.5 ± 2.6 mV vs. SCE, respectively. The value of $E_{f,2}$ was close to both formal potentials derived from first derivatives of CV under turnover conditions (see Fig. 2). This could indicate that the redox couple detected at $E_{f,2}$ was responsible for the bioelectrocatalytic electron transfer.

Nevertheless, the lack of an electrochemical characterization of the OMCs of *Glk. subterraneus* prohibits an *a priori* assignment of $E_{f,2}$ to a certain type of protein (or multiple proteins) responsible for the suggested DET mechanism.

2.3.1 Non-turnover CV comparison of *Geoalkalibacter subterraneus* and *Geobacter sulfurreducens* biofilms

Further data supporting a putative DET by *Glk. subterraneus* comes from the comparison of its non-turnover CV with the one obtained with *Gb. sulfurreducens* biofilms. Although non-turnover CVs of *Glk. subterraneus* (with two redox systems) and *Gb. sulfurreducens* (with four redox couples previously observed[27, 51]) differed significantly (see Fig. S4), the value of *Glk. subterraneus*'s formal potential $E_{f,2}$ was close to *Gb. sulfurreducens*'s $E_{f,Gb2}$. This suggests a common DET mechanism in both bacteria. Based on this experimental data and on previous studies of *Gb. sulfurreducens* that propose a DET via OMCs[63], we suggest to ascribe the formal potential $E_{f,2}$ found here for *Glk. subterraneus* to a DET very likely via an OMC. Future research should therefore concentrate on the investigation of the OMC (or OMCs) involved in the DET mechanism of *Glk. subterraneus*.

The proper assignation of $E_{f,4}$ to a respective ET mechanism (Fig. 3B) was not a straightforward task. Some authors previously suggested a possible explanation based on the CV observed for *Gb. sulfurreducens* biofilms[27, 51]. Here we propose to extrapolate such explanation derived from the comparison of Fig. 2B and 3B to our results. From these figures one can see that $E_{f,1}$, $E_{f,2}$ and $E_{f,3}$ share a very similar value. Therefore, it can be hypothesized that these redox processes contributed to the bioelectrocatalytic anodic electron transfer. On the other hand, since $E_{f,4}$ does not have a formal potential match in turnover conditions, it appears to have no contribution in the overall ET mechanism.

2.4 Imaging of *Geoalkalibacter subterraneus* biofilm surface coverage and thickness using confocal laser scanning microscopy

In order to study how *Glk. subterraneus* (and *Gb. sulfurreducens* for comparison) attached to the electrode surface, confocal laser scanning microscopy (CLSM) was used to conduct a qualitative (with LAS AF and Volocity®) description and a quantitative (with PHLIP) biofilm analysis as described in the Experimental section. In this course, it has to be noticed that this is the first CLSM description of *Glk. subterraneus* electroactive biofilms. CLSM was used first of all, for its advantage over Scanning electron microscopy for quantitatively analyzing in depth the layers across the biofilm and hence, allowing the calculation of surface coverage and thickness[64]. Second, CLSM allows a live biofilm to be imaged by avoiding a harsh drying

procedure that could change its morphology. In our experiments the biofilms were stained with a LIVE/DEAD® kit. Bacterial cells embed in biofilms stained green which could indicate that most of the cells were still metabolically active at the moment of the CLSM analysis[17]. However, since this is the first work reporting the use of this kit with biofilms of *Glk. subterraneus*, the successful staining of dead cells of this bacterium should be still experimentally tested. The maximum intensity projection of a *Glk. subterraneus* biofilm is shown in Fig. 4A. This picture confirms a very uniform coverage of the electrode surface as previously observed by visual inspection of a reddish biofilm (see Fig. S5). Additionally, when analyzing the different slices that compose the maximum intensity projection, it is clear that the biofilm was constituted of a stack of several biofilm monolayers (see Fig. S6). From the different orthogonal cross sections made throughout the biofilm, it seems that the biofilm is about 30 µm thick (Fig. 4B). However, this idea was later discarded by PHLIP quantitative analysis which showed a biofilm with a thickness value of 76 ± 7 µm as described in the following section. Further 3D reconstruction with Volocity® revealed a very peculiar biofilm structure (see Fig. S7) composed of an undulating structure distributed across the analyzed electrode surface sample probably caused by biofilm overgrown which matches previous observations in *Gb. sulfurreducens* biofilms[17, 51].

2.4.1 CLSM comparison of *Geoalkalibacter subterraneus* and *Geobacter sulfurreducens* biofilms

The comparison of *Glk. subterraneus* and *Gb. sulfurreducens* CLSM pictures is shown in Fig. S8 and in Table S3. It was observed that *Glk. subterraneus* produced a lower current density (4.68 ± 0.54 A/m^2) when it formed a thicker biofilm (76 ± 7 µm) than *Gb. sulfurreducens*. Nevertheless, the average electrode coverage value of *Gb. sulfurreducens* (31 ± 16 %) is higher than the one of *Glk. subterraneus* (23 ± 7 %) and therefore indicating that these differences in biofilm architecture contribute to explain the higher current density by *Gb. sulfurreducens*. A similar trend was recently reported by Richter *et al.*[65]. They studied *Gb. sulfurreducens* wild-type and the mutant *pilA4*, a strain expressing only the short isoform of the PilA preprotein that composes the type IV pili of *Gb. sulfurreducens*, a protein essential for DET. Therefore, diminishing the ability of the mutant to effectively transfer electrons to insoluble Fe(III) oxides and graphite anodes. Whereas the wild-type of *Gb. sulfurreducens* produced a higher current density, it showed a thinner biofilm but higher electrode coverage value than the mutant.

One issue that emerges from the thickness observed in *Glk. subterraneus* is that the value is very high for the values normally reported in the literature for pure culture electroactive bacteria[14-18]. Thus, to be the first CLSM description of this strain, it is advisable and justifiable to further investigate the possible reasons behind the biofilms produced by this electroactive bacterial species.

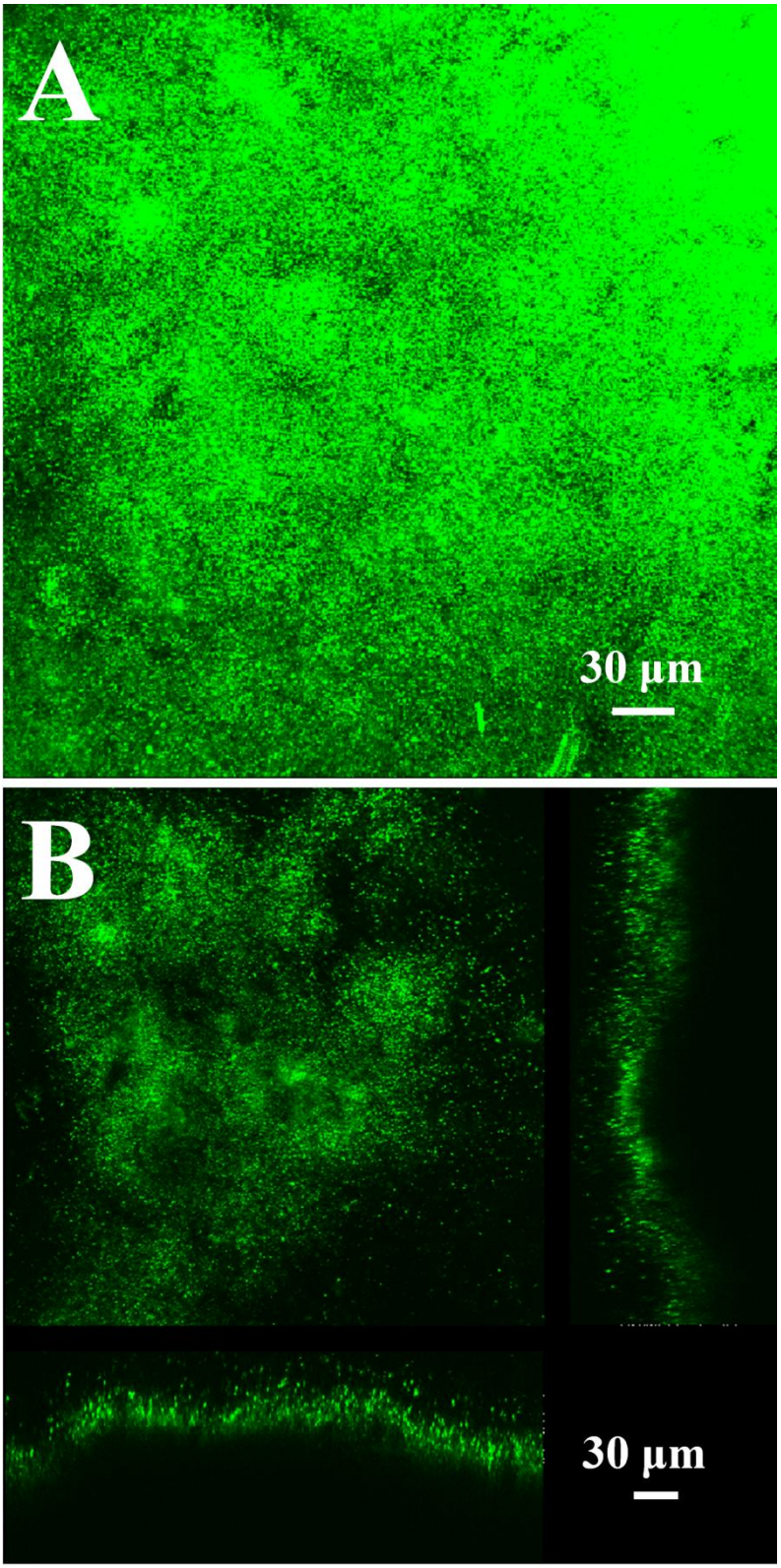

Fig. 4 Exemplary confocal laser scanning microscopy of *Geoalkalibacter subterraneus* biofilms grown on graphite planar electrodes. A) Maximum intensity projection and B) Orthogonal cross section of a single slice through the biofilm with top and right panels representing perpendicular slices.

2.4.2 Proof that the presence of an electroactive biofilm is due to metabolically active bacterial cells transferring electrons to the electrode

To support that the biofilm formation was due to the electrons harvested from the substrate oxidation followed by a later release to the electrode surface by the electroactive biofilm, CLSM images were compared to a non-electrochemical negative control. This control was an electrode placed in the same electrochemical cell of a *Glk. subterraneus* electrochemical experiment but not potentiostatically controlled (*i.e.*, the electrode was immersed in the same growth medium during the electrochemical biofilm growth). The result of such CLSM observations is shown in Fig. S8 and Table S3. When comparing CLSM pictures in Fig. S8, the difference between both maximum intensity projections and orthogonal cross sections is very clear. While for the potentiostatically controlled electrode there was an evident thick biofilm formed of metabolically active bacteria, for the negative control no significant coverage of the electrode surface and biofilm formation was observed (see Table S3). These findings are consistent with the observations made by Malvankar *et al.* (2011)[66]. They utilized in a similar way a non-connected electrode as negative control electrode. The values of electrode coverage and thickness calculated here for the negative control electrode suggest that the bacterial cells stained with the LIVE/DEAD kit corresponded to a heterogenous deposition of bacterial cells likely de-attached from the potentiostatically controlled electrode in which *Glk. subterraneus* was forming an electroactive biofilm (Fig. S8).

These CLSM findings are well in line with previous studies of ARB able to produce high currents and thick biofilms such as *Geobacter sulfurreducens*[15, 17, 29, 51, 66] and *Thermincola ferriacetica*[22] but in clear contrast to other low current producing bacteria like *Shewanella* species[19]. On the other side, similar observations of biofilm coverage of an electrode material were obtained with Scanning electron microscopy measurements in *Rhodopseudomonas palustris* DX-1[40], *Geoalkalibacter ferrihydriticus*[30] and *Geolkalibacter subterraneus*[30].

3 Conclusions

The present study on the characterization of *Geoalkalibacter subterraneus* is summarized in Fig. 5 and indicates the following findings: CA exhibited the highest current density (4.68 ± 0.54 A/m^2) produced on a planar electrode for a pure culture of an ARB under saline conditions (3.5% NaCl). CV under turnover and non-turnover conditions made evident the appearance of two different redox couples for each condition. When comparing their formal potentials, two of them had a very close value ($E_{f,2}$ and $E_{f,3}$) indicating that the molecule (or molecules) responsible for the ET mechanism might fall between the potential window delimited by $E_{f,2}$ and $E_{f,3}$. CLSM confirmed a biofilm composed of several layers of metabolically active bacteria that spread all over the electrode material with a thick biofilm up to 76 ± 7 μm height but a low electrode coverage of only 23 ± 7 %. From these findings, it is then proposed that *Geoalkalibacter subterraneus* performs a DET mechanism in contact with the electrode material. Nevertheless, to firmly determine the molecule responsible for the ET mechanism future work will be performed by employing Surface Enhanced Resonance Raman Spectroscopy, a technique successfully used to detect selectively cellular membrane redox proteins in proximity of the electrode surface[63, 67, 68].

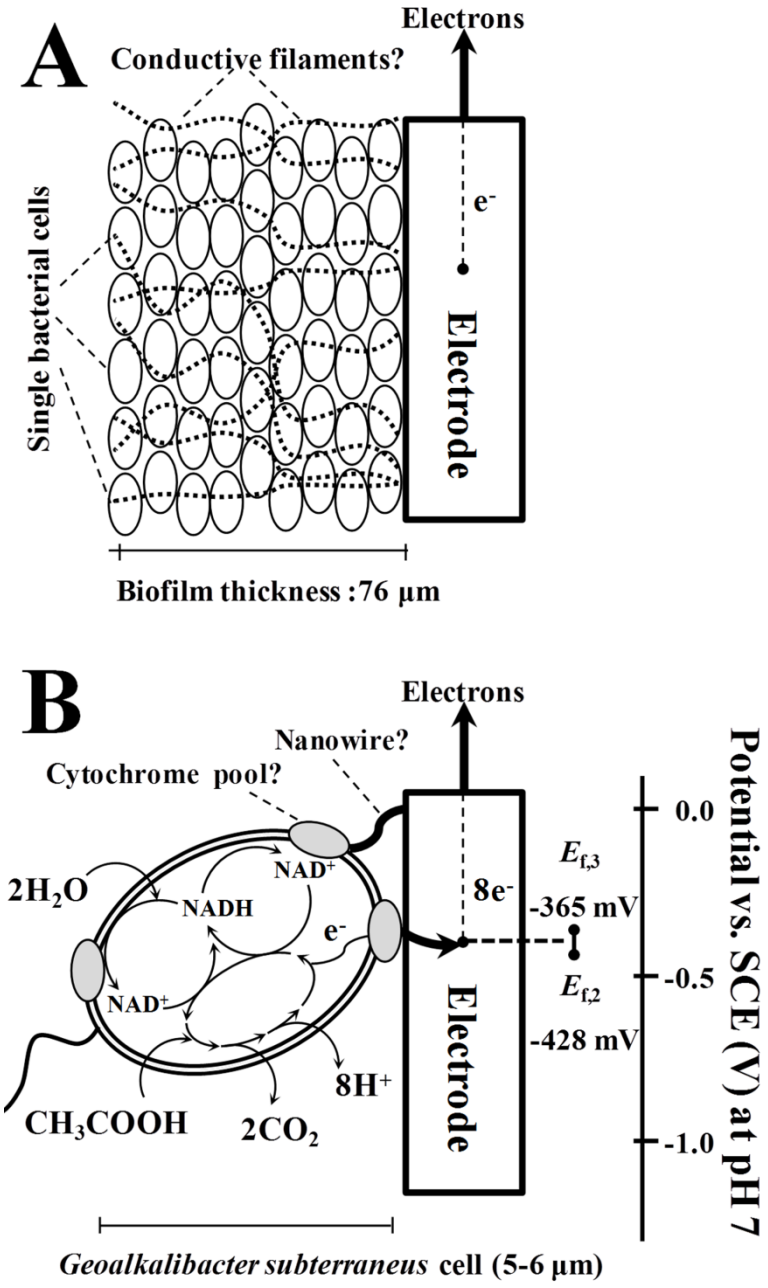

Fig. 5 Conceptual illustration of the DET mechanism performed by *Geoalkalibacter subterraneus* derived from the electrochemical and microscopic characterization accomplished here. A) Representation of the visible apparent biofilm with a 70-80 µm thickness that could possibly contain conductive filaments[30] to transport electrons by the so called long-range ET[69] through the biofilm composed of monolayers of stained green cells as per CLSM analysis; B) Schematic proposal at the single cell level[26] accomplishing the oxidation of acetate to produce carbon dioxide and harvest of electrons, for instance, by the tricarboxylic acid cycle[70] to perform a DET mechanism via a putative cytochrome (or cytochrome pool) with a formal potential "conduit" (E_f) between -428 and -365 mV vs. SCE determined during CV analysis.

4 Experimental

4.1 General conditions

All chemicals were of analytical or biochemical grade and were purchased from Sigma-Aldrich and Merck. If not stated otherwise, all potentials provided in this manuscript refer to the SCE reference electrode (KCl 3.0 M, +240 mV vs. SHE, Materials Mates, La Guilletière 38700 Sarcenas, France). All media preparations were adjusted to pH 7, vigorously flushed with N_2 gas (purity ≥ 99.9999, Linde France S.A.) for at least 30 min using a commercial air stone (or aquarium bubbler) and then autoclaved (121°C for 20 min). Bioelectrochemical experiments were conducted under potentiostatic control and strictly anoxic[71, 72] and sterile conditions. All incubations were performed at 37°C.

4.2 Metabolite and biogas analysis

Acetate consumption was determined by liquid injection into a gas chromatograph (GC 8000, Fisons Instruments) according to Aceves-Lara *et al.*, 2008[73]. Biogas composition (CH_4, CO_2, H_2 and N_2) was determined using a gas chromatograph (Clarus 580, Perkin Elmer) coupled to Thermal Catharometric detection, as described elsewhere[74].

4.3 Cell cultures and media

Geoalkalibacter subterraneus strain Red1 was purchased from DSMZ (DSM No.: 23483, German Collection of Microorganisms and Cell Cultures GmbH, Braunschweig, Germany). Sterile growth medium FRR[26] was used for routinely culture maintenance and contained (per L): 17.0 g of NaCl, 4.50 g of $MgCl_2 \cdot 6H_2O$, 0.35 g of $CaCl_2 \cdot 2H_2O$, 1.00 g of NH_4Cl, 0.08 g KH_2PO_4, 3.50 g of $NaHCO_3$, 3.00 g of Yeast extract, 1 mL of trace element solution, 1 mL of selenite-tungstate solution, 2.55 g of $NaNO_3$ as final electron acceptor when *Glk. subterraneus* cells were harvested for further growth in electrochemical cells (as described below) and 1.00 g of CH_3COONa as electron donor.

As stated before, the novel ARB *Glk. subterraneus* was the bacterium dominating high current producing biofilms in previous studies of our group[31]. Therefore, for the growth of *Glk. subterraneus* biofilms on graphite electrodes (*i.e.*, in electrochemical experiments) two similar media compositions were used. Medium FRR[26] without $NaNO_3$ and modified Starkey medium as reported elsewhere[75] were used. The later was used previously for the selection and identification of *Glk. subterraneus* in a potentiostically controlled BES[31]. Starkey medium contained per liter: 35.0 g NaCl, 0.5 g K_2HPO_4, 2.0 g NH_4Cl, 7.6 g MES buffer, 0.2 g Yeast Extract, 1 mL of oligo-elements solution and 10 mM sodium acetate as electron donor. Oligo-elements solution contained (per L): 46 mL HCl 37%, 55 g $MgCl_2 \cdot 6H_2O$, 7.0 g

$FeSO_4(NH_4)_2SO_4 \cdot 6H_2O$, 1.0 g $ZnCl_2 \cdot 2H_2O$, 1.2 g $MnCl_2 \cdot 4H_2O$, 0.4 g $CuSO_4 \cdot 5H_2O$, 1.3 g $CoSO_4 \cdot 7H_2O$, 0.1 g BO_3H_3, 1.0 g $Mo_7O_{24}(NH_4)_6 \cdot 4H_2O$, 0.05 g $NiCl_2 \cdot 6H_2O$, 0.01 g $Na_2SeO_3 \cdot 5H_2O$ and 60.0 g $CaCl_2 \cdot 2H_2O$. The examination of the two media in electrochemical experiments inoculated with *Glk. subterraneus* led to similar performance (see Fig.S1 and Table S2).

As stated before, to conduct an accurate comparison of the performance obtained with *Glk. subterraneus*, parallel electrochemical experiments were carried out with *Gb. sulfurreducens* (DSM strain number 12127). *Gb. sulfurreducens* cells were harvested for electrochemical experiments as reported elsewhere[28, 60, 76], except during growth on graphite electrodes. In experiments reported here with *Gb. sulfurreducens*, no gas was flushed during the growth of biofilms in electrochemical experiments.

4.4 Electrode preparation

Preparation of electrodes was according to the procedure reported elsewhere[77]. In brief: working electrodes were 2.5 cm x 2.5 cm x 0.25 cm (total immersed projected electrode surface area of 15 cm^2) planar graphite plates (C000440/15, Goodfellow SARL, 229 Rue Solférino, F-59000 Lille, France) screwed onto 2 mm diameter, 15 cm long titanium rods (TI007910/13, Goodfellow) that ensured electrical connection. Planar graphite electrodes were used as delivered by the provider. Counter electrodes were 90% Platinum-10% Iridium grids joint by heating in a blue flame with a 0.5 mm diameter, 15 cm long 90% Platinum-10% Iridium rod (Heraeus PSP S.A.S., Contact Materials Division, 526, Route des Gorges du Sierroz, 73100 Grésy-sur-Aix France).

4.5 Bioelectrochemical set-up and experiments

Glk. subterraneus and *Gb. sulfurreducens* biofilms were grown in potentiostatically controlled half-cells (autoclavable borosilicate glass) containing 500 mL of solution with around 200 mL of headspace as reported elsewhere[77]. The lid and the reactor body were sealed with a clamping ring. Biofilm growth was performed in semi-batch chronoamperometric (CA) experiments with media replacement as described previously[19] at a fixed applied potential of +200 mV using a Potentiostat/Galvanostat VMP3 (BioLogic Science Instruments, France). After half-cells containing electrodes were completely assembled (*i.e.*, before inoculation of bacterial cells) anoxic conditions were assured similarly as in previous reports[28, 60, 76]. Here, we flushed the media with high purity N_2 ($\geq$ 99.9999 %) for at least 30 min. The final composition of the gas phase was typically a mixture of O_2: 1.41 ± 1.16 % and N_2: 98.56 ± 1.18 %.

Inoculation of bacterial cells was carried out as previously described[19]. Concisely, 50 mL of media in the early stationary phase (i.e., OD^{620} approx. 0.3-0.4) were anoxically sampled[71, 72] and centrifuged at 3000 rpm for 10 min. The pellet was re-suspended in 10 mL of the respective media for electrochemical experiments and injected in the electrochemical cell (see Fig. S9).

4.6 Cyclic voltammetry (CV) for an insight into the electron transfer (ET) mechanism

Different types of CVs were recorded during experiments according to Refs.[19, 27, 78] (see Fig. 1). Control CV of the bare graphite electrode immersed in growth media before starting CA and inoculating the half-cell (dotted line in Fig. 2A), turnover CV of a *Glk. subterraneus* biofilm, *i.e*. at bioelectrocatalytic substrate consumption (continuous line in Fig. 2A) and two types of non-turnover CV of a *Glk. subterraneus* biofilm: during substrate depleted conditions (continuous line in Fig. 3A) and during substrate deprived conditions (continuous line in Fig. 3B).

4.7 Data processing

CA maximum current densities (j_{max}) of established microbial biofilms were analyzed considering the total immersed electrode surface area since electroactive biofilms covered both sides of the working electrode as per our observations (*i.e*., not only the side of graphite working electrode facing Pt-Ir counter electrode, see Fig. S5). Here all data are based on experiments of at least two independent biofilm replicates[79] and standard deviations are presented through all the manuscript. For in-depth data analyses of CV, the open–source software SOAS[62] was used for baseline (capacitive current) correction for non-turnover conditions.

4.8 Confocal laser scanning microscopy (CLSM) to measure biofilm electrode coverage and thickness

Glk. subterraneus biofilms (and *Gb. sulfurreducens* for comparison) grown on planar graphite plate electrodes were examined by CLSM after staining with nucleic acid-specific fluorochromes. For this purpose, whole electrodes were mounted on a plastic petri dish and subsequently stained with the LIVE/DEAD® BacLight™ Bacterial Viability Kit (Invitrogen) as proposed by the manufacturer. Stained biofilms were covered with tap water and confocal images of electroactive biofilms were acquired with a confocal laser scanning system (Leica TCS SP2, Leica Microsystems, Wetzlar, Germany) using a 40x water immersion objective (numerical aperture 0.8). Biofilms were observed with the 488 nm ray line of an argon laser for excitation and the emitted light was collected in the 495- 616 nm spectral range. The

system was controlled by the Leica LCS software (version 2.61) (Leica, Germany). Each electroactive biofilm attached to the electrode was scanned for CLSM images at three different random locations; therefore, CLSM images were representative of the entire electrode. These images were qualitatively inspected (LAS AF 2.4.1 build 6384, Leica Microsystems and Volocity® Demo Version 6.2.1[80], PerkinElmer). Images were later thresholded at 60[81] and quantitatively analyzed with PHobia Laser scanning microscopy Imaging Processor 0.3 (PHLIP)[82], an open source public license Matlab toolbox commonly used for the analysis of electroactive biofilms[15, 65, 66].

5 Acknowledgments

This research was financed by the French National Research Agency (ANR-09-BioE-10 DéfiH12). The authors gratefully acknowledge C. Pouzet and A. Le Ru for technical assistance with CLSM. A.A.C.M thanks E. Latrille, V. Rossard and L. Dantas for help with Matlab/PHLIP and Linux/SOAS software handling and C. Rivalland for critical reading of the manuscript.

6 References

1. S. Patil, C. Hägerhäll and L. Gorton, *Bioanal. Rev.*, 2012, **4**, 159-192.
2. B. E. Logan, B. Hamelers, R. Rozendal, U. Schröder, J. Keller, S. Freguia, P. Aelterman, W. Verstraete and K. Rabaey, *Environ. Sci. Technol.*, 2006, **40**, 5181-5192.
3. B. E. Logan, D. Call, S. Cheng, H. V. M. Hamelers, T. H. J. A. Sleutels, A. W. Jeremiasse and R. A. Rozendal, *Environ. Sci. Technol.*, 2008, **42**, 8630-8640.
4. K. Rabaey and R. A. Rozendal, *Nat. Rev. Micro.*, 2010, **8**, 706-716.
5. D. R. Lovley, *Energy Environ. Sci.*, 2011, **4**, 4896-4906.
6. A. A. Carmona-Martínez, F. Harnisch, L. A. Fitzgerald, J. C. Biffinger, B. R. Ringeisen and U. Schröder, *Bioelectrochemistry*, 2011, **81**, 74-80.
7. K. Rabaey, N. Boon, M. Höfte and W. Verstraete, *Environ. Sci. Technol.*, 2005, **39**, 3401-3408.
8. E. Marsili and X. Zhang, in *Bioelectrochemical Systems: from Extracellular Electron Transfer to Biotechnological Application*, eds. K. Rabaey, L. Angenent, U. Schroder and J. Keller, 2010, pp. 59-80.
9. M. E. Hernandez and D. K. Newman, *Cell. Mol. Life Sci.*, 2001, **58**, 1562-1571.
10. U. Schröder, *Phys. Chem. Chem. Phys.*, 2007, **9**, 2619-2629.
11. K. Watanabe, M. Manefield, M. Lee and A. Kouzuma, *Curr. Opin. Biotechnol.*, 2009, **20**, 633-641.
12. K. P. Katuri, S. Rengaraj, P. Kavanagh, V. O'Flaherty and D. Leech, *Langmuir*, 2012, **28**, 7904-7913.
13. G. Reguera, K. P. Nevin, J. S. Nicoll, S. F. Covalla, T. L. Woodard and D. R. Lovley, *Appl. Environ. Microbiol.*, 2006, **72**, 7345-7348.
14. A. E. Franks, R. H. Glaven and D. R. Lovley, *ChemSusChem*, **5**, 1092-1098.
15. A. E. Franks, K. P. Nevin, H. Jia, M. Izallalen, T. L. Woodard and D. R. Lovley, *Energy Environ. Sci.*, 2009, **2**, 113-119.
16. A. E. Franks, K. P. Nevin, R. H. Glaven and D. R. Lovley, *ISME J*, 2010, **4**, 509-519.
17. K. P. Nevin, H. Richter, S. F. Covalla, J. P. Johnson, T. L. Woodard, A. L. Orloff, H. Jia, M. Zhang and D. R. Lovley, *Environ. Microbiol.*, 2008, **10**, 2505-2514.
18. K. P. Nevin, B.-C. Kim, R. H. Glaven, J. P. Johnson, T. L. Woodard, B. A. Methé, R. J. DiDonato, Jr., S. F. Covalla, A. E. Franks, A. Liu and D. R. Lovley, *PLoS ONE*, 2009, **4**, e5628.
19. A. A. Carmona-Martínez, F. Harnisch, U. Kuhlicke, T. R. Neu and U. Schröder, *Bioelectrochemistry*, 2012.
20. A. Okamoto, R. Nakamura and K. Hashimoto, *Electrochim. Acta*, 2011, **56**, 5526-5531.
21. A. Jain, X. Zhang, G. Pastorella, J. O. Connolly, N. Barry, R. Woolley, S. Krishnamurthy and E. Marsili, *Bioelectrochemistry*, 2013, **87**, 28-32.
22. P. Parameswaran, T. Bry, S. Popat, B. G. Lusk, B. E. Rittmann and C. I. Torres, *Environ. Sci. Technol.*, 2013. **47**, 4934-4940.
23. C. I. Torres, A. K. Marcus, H. S. Lee, P. Parameswaran, R. Krajmalnik-Brown and B. E. Rittmann, *FEMS Microbiol. Rev.*, 2010, **34**, 3-17.
24. F. Harnisch and K. Rabaey, *ChemSusChem*, 2012, **5**, 1027-1038.
25. M. Pierra, *Commun. Agric. Appl. Biol. Sci.*, 2012, **77**, 58.
26. A. C. Greene, B. K. C. Patel and S. Yacob, *Int. J. Syst. Evol. Microbiol.*, 2009, **59**, 781-785.
27. K. Fricke, F. Harnisch and U. Schroder, *Energy Environ. Sci.*, 2008, **1**, 144-147.
28. C. Dumas, R. g. Basseguy and A. Bergel, *Electrochim. Acta*, 2008, **53**, 3200-3209.
29. H. Richter, K. McCarthy, K. P. Nevin, J. P. Johnson, V. M. Rotello and D. R. Lovley, *Langmuir*, 2008, **24**, 4376-4379.
30. J. P. Badalamenti, R. Krajmalnik-Brown and C. I. Torres, *mBio*, 2013, **4**.
31. M. Pierra, E. Trably, J.-J. Godon and N. Bernet, unpublished work.
32. J. F. Miceli, P. Parameswaran, D.-W. Kang, R. Krajmalnik-Brown and C. I. Torres, *Environ. Sci. Technol.*, 2012, **46**, 10349-10355.
33. O. Lefebvre, Z. Tan, S. Kharkwal and H. Y. Ng, *Bioresour. Technol.*, 2012, **112**, 336-340.
34. S. Cheng, H. Liu and B. E. Logan, *Environ. Sci. Technol.*, 2006, **40**, 2426-2432.
35. H. Liu, R. Ramnarayanan and B. E. Logan, *Environ. Sci. Technol.*, 2004, **38**, 2281-2285.

36. H. Liu, S. Cheng and B. E. Logan, *Environ. Sci. Technol.*, 2005, **39**, 658-662.
37. E. Lalaurette, S. Thammannagowda, A. Mohagheghi, P.-C. Maness and B. E. Logan, *Int. J. Hydrogen Energy*, 2009, **34**, 6201-6210.
38. D. R. Bond and D. R. Lovley, *Appl. Environ. Microbiol.*, 2003, **69**, 1548-1555.
39. L. Zhu, H. Chen, L. Huang, J. Cai and Z. Xu, *Eng. Life Sci.*, 2011, **11**, 238-244.
40. D. Xing, Y. Zuo, S. Cheng, J. M. Regan and B. E. Logan, *Environ. Sci. Technol.*, 2008, **42**, 4146-4151.
41. C. W. Marshall and H. D. May, *Energy Environ. Sci.*, 2009, **2**, 699-705.
42. S. Xu and H. Liu, *J. Appl. Microbiology*, 2011, **111**, 1108-1115.
43. D. Xing, S. Cheng, B. Logan and J. Regan, *Appl. Microbiol. Biotechnol.*, 2010, **85**, 1575-1587.
44. S. K. Chaudhuri and D. R. Lovley, *Nat. Biotech.*, 2003, **21**, 1229-1232.
45. B. E. Logan and J. M. Regan, *Trends Microbiol.*, 2006, **14**, 512-518.
46. A. E. Inglesby, D. A. Beatty and A. C. Fisher, *RSC Advances*, 2012, **2**, 4829-4838.
47. B.-Y. Chen, Y.-M. Wang and I. S. Ng, *Bioresour. Technol.*, 2011, **102**, 1159-1165.
48. T. Zhang, L. Zhang, W. Su, P. Gao, D. Li, X. He and Y. Zhang, *Bioresour. Technol.*, 2011, **102**, 7099-7102.
49. Y. Yuan, J. Ahmed, L. Zhou, B. Zhao and S. Kim, *Biosens. Bioelectron.*, 2011, **27**, 106-112.
50. D. E. Holmes, D. R. Bond and D. R. Lovley, *Appl. Environ. Microbiol.*, 2004, **70**, 1234-1237.
51. A. Jain, G. Gazzola, A. Panzera, M. Zanoni and E. Marsili, *Electrochim. Acta*, 2011, **56**, 10776-10785.
52. J. Niessen, U. Schröder, F. Harnisch and F. Scholz, *Lett. Appl. Microbiol.*, 2005, **41**, 286-290.
53. X. Zhu, M. D. Yates and B. E. Logan, *Electrochem. Commun.*, 2012, **22**, 116-119.
54. S. M. Strycharz, A. P. Malanoski, R. M. Snider, H. Yi, D. R. Lovley and L. M. Tender, *Energy Environ. Sci.*, 2011, **4**, 896-913.
55. K. P. Katuri, P. Kavanagh, S. Rengaraj and D. Leech, *Chem. Commun.*, 2010, **46**, 4758-4760.
56. J. Wei, P. Liang, X. Cao and X. Huang, *Environ. Sci. Technol.*, 2010, **44**, 3187-3191.
57. E. Marsili, J. Sun and D. R. Bond, *Electroanalysis*, 2010, **22**, 865-874.
58. H. Richter, K. P. Nevin, H. Jia, D. A. Lowy, D. R. Lovley and L. M. Tender, *Energy Environ. Sci.* 2009, **2**, 506-516.
59. S. Srikanth, E. Marsili, M. C. Flickinger and D. R. Bond, *Biotechnol. Bioeng.*, 2008, **99**, 1065-1073.
60. C. Dumas, R. Basseguy and A. Bergel, *Electrochim. Acta*, 2008, **53**, 2494-2500.
61. E. Marsili, J. B. Rollefson, D. B. Baron, R. M. Hozalski and D. R. Bond, *Appl. Environ. Microbiol.*, 2008, **74**, 7329-7337.
62. V. Fourmond, K. Hoke, H. A. Heering, C. Baffert, F. Leroux, P. Bertrand and C. Léger, *Bioelectrochemistry*, 2009, **76**, 141-147.
63. D. Millo, F. Harnisch, S. A. Patil, H. K. Ly, U. Schröder and P. Hildebrandt, *Angew. Chem., Int. Ed.*, 2011, **50**, 2625-2627.
64. A. E. Franks, N. Malvankar and K. P. Nevin, *Biofuels*, 2010, **1**, 589-604.
65. L. V. Richter, S. J. Sandler and R. M. Weis, *J. Bacteriol.*, 2012, **194**, 2551-2563.
66. N. S. Malvankar, M. Vargas, K. P. Nevin, A. E. Franks, C. Leang, B.-C. Kim, K. Inoue, T. Mester, S. F. Covalla, J. P. Johnson, V. M. Rotello, M. T. Tuominen and D. R. Lovley, *Nat. Nanotechnol.*, 2011, **6**, 573-579.
67. H. K. Ly, F. Harnisch, S.-F. Hong, U. Schröder, P. Hildebrandt and D. Millo, *ChemSusChem*, 2013, **6**, 487-492.
68. D. Millo, *Bioanal. Rev.*, 2012, **40**, 1284-1290.
69. N. S. Malvankar and D. R. Lovley, *ChemSusChem*, 2012, **5**, 1039-1046.
70. D. R. Lovley, *Nat Rev Micro*, 2006, **4**, 497-508.
71. T. L. Miller and M. J. Wolin, *J. Appl. Microbiol.*, 1974, **27**, 985-987.
72. R. E. Hungate and J. Macy, *Bulletins from the Ecological Research Committee*, 1973, 123-126.
73. C. s. A. Aceves-Lara, E. Latrille, P. Buffiere, N. Bernet and J.-P. Steyer, *Chem. Eng. Process. Process Intensif.*, 2008, **47**, 1968-1975.
74. M. Quéméneur, J. Hamelin, A. Barakat, J.-P. Steyer, H. Carrère and E. Trably, *Int. J. Hydrogen Energy*, 2012, **37**, 3150-3159.

75. Y. Rafrafi, E. Trably, J. Hamelin, E. Latrille, I. Meynial-Salles, S. Benomar, M.-T. Giudici-Orticoni and J.-P. Steyer, *Int. J. Hydrogen Energy*, 2013.
76. C. Dumas, R. g. Basseguy and A. Bergel, *Electrochim. Acta*, 2008, **53**, 5235-5241.
77. S. F. Ketep, A. Bergel, M. Bertrand, W. Achouak and E. Fourest, *Bioresour. Technol.*, 2013, **127**, 448-455.
78. F. Harnisch and S. Freguia, *Chem. Asian J.*, 2012, **7**, 466-475.
79. B. E. Logan, *ChemSusChem*, 2012, **5**, 988-994.
80. S. Beaufort, S. Alfenore and C. Lafforgue, *J. Membr. Sci.*, 2011, **369**, 30-39.
81. X. Yang, H. Beyenal, G. Harkin and Z. Lewandowski, *Water Res.*, 2001, **35**, 1149-1158.
82. L. Mueller, J. de Brouwer, J. Almeida, L. Stal and J. Xavier, *BMC Ecology*, 2006, **6**, 1.